Q. J. R. Meteorol. Soc. (2000), **126**, pp. 111–123

Convective destabilization by upper-level troughs

By MARTIN JUCKES and ROGER K. SMITH*
Meteorological Institute, University of Munich

(Received 14 December 1998; revised 12 May 1999)

SUMMARY

The approach of an upper-level trough is accompanied by a local ascent of the isentropic surfaces in the troposphere. The associated cooling and moistening destabilizes the atmosphere to convection. In this paper we attempt to quantify the maximum amount of destabilization as a function of the amplitude and horizontal scale of the trough. The trough is represented by an elongated potential-temperature perturbation on the tropopause. Its structure, including the isentrope displacement it produces, is calculated from the balanced shear-line solutions of Juckes. These solutions are used to estimate the amount by which mid- and lower-tropospheric air masses are lifted when an upper-tropospheric trough passes overhead on the assumption that isentropic potential-vorticity anomalies are localized in the upper troposphere. The amount of destabilization is characterized by the maximum change in convective available potential energy (CAPE) and convective inhibition (CIN) brought about by the passage of the trough. The calculations seek to isolate one aspect of the interaction between an upper-level trough and a tropical cyclone. We show that the changes in CAPE are significant in the Tropics (up to 83% for the soundings examined) and even more so in the middle latitudes (up to 130%) and that the CIN may be completely removed.

KEYWORDS: Convective destabilization Potential vorticity Tropopause Upper-level troughs

1. INTRODUCTION

The mutual approach of an upper-level trough† and a tropical cyclone is frequently accompanied by significant intensification or weakening of the cyclone. These intensity changes are notoriously difficult to predict. The observations suggest that there is a two-way interaction between the trough and the cyclone, which has been hypothesized to result from the superposition of a cyclonic upper-level potential-vorticity (PV) anomaly (the trough) and a cyclonic lower-level PV anomaly (the tropical cyclone), together with the negative PV anomaly of the tropical-cyclone outflow layer. The sequence of events includes changes in vertical shear over the storm, fluctuations in the distribution and intensity of convection, and alterations in the structure of the trough itself. The physical mechanisms underlying these events are multi-scale and are not well established. In particular, the links between the large-scale flow and the inner core of the tropical cyclone are poorly understood. The current state of knowledge is summarized in the papers by Molinari *et al.* (1995, 1998). Generally the interaction is thought to have a positive influence on intensification, although the vertical shear associated with the trough is believed to play a role in weakening the cyclone. One aspect of a moving trough that might lead to intensification is the convective destabilization brought about through the lifting of the isentropes throughout the troposphere (see Hoskins *et al.* 1985). There are two conceptually (and spatially) distinct processes through which the isentropic lifting can lead to latent-heat release. In mid-latitudes it is often the large-scale upward motion which is of greatest importance. Coherent upward motion typically occurs on that side of the cyclonic anomaly to which the thermal-wind vector of the large-scale flow points (Eliassen and Kleinschmidt 1957, chapter IV). Here we are concerned not with the maximum anomaly-scale upward motion, but rather with the maximum upward displacements on the anomaly-scale. These occur at the centre of the upper-cyclonic anomaly. The displacements lead to cooling and normally to a moistening at a given height, thereby increasing the convective available potential

* Corresponding author: Meteorological Institute, University of Munich, Theresienstr. 37, 80333 Munich, Germany.

† A trough is defined here as an elongated cyclonic potential-vorticity anomaly.

energy (CAPE) and reducing the convective inhibition (CIN)*. This paper seeks to quantify the degree of convective destabilization that may be brought about by the approach of the trough by evaluating the changes in CAPE and CIN as a function of trough size and strength for typical environmental temperature and humidity soundings. The calculations are of particular interest as many convective parametrization schemes relate the intensity of convection to the amount of grid-scale CAPE.

2. THE UPPER TROUGH

Juckes (1999) describes an algorithm for determining the structure of shear lines associated with upper-tropospheric anomalies which are created by the advection of potential-temperature anomalies along the dynamical tropopause. The dynamical tropopause is defined as a surface of constant potential vorticity (Reed 1955; Danielsen 1968). It has the advantage that it is a material surface under adiabatic conditions. Since the creation of upper-level troughs takes place largely through meridional advection, the structure of the dynamical tropopause provides a useful description of the flow. The dynamical tropopause generally slopes downwards towards the poles, and also has a lower potential temperature at high latitudes. As air is advected equatorwards, a cold anomaly in tropopause potential temperature is created. During the advection process an ageostrophic circulation acts to keep the structure of the upper-level trough balanced. It is possible to deduce the final balanced structure of the trough from the amplitude of the potential-temperature anomaly on the tropopause and the potential-vorticity structure within the stratosphere and troposphere, without following all the details of its formation.

Two simplifying assumptions are made so as to facilitate the calculation of a range of trough structures. Firstly, the flow is taken to be two dimensional. This allows a steady balanced structure to be calculated, which is an exact solution of the primitive equation to within numerical accuracy. Secondly, it is assumed that the isentropic gradients of potential vorticity vanish both within the stratosphere and troposphere. The only place where isentropic gradients occur is where the isentropes intersect the tropopause. It follows that the relation between potential vorticity and potential temperature can be expressed in terms of two functions, $P_s(\theta)$ and $P_t(\theta)$, which specify the value of the potential vorticity on an isentrope with potential temperature θ in the stratosphere or troposphere, respectively. The potential vorticity P is defined as $P = -g(f + \mathbf{k} \cdot \nabla_\theta \times \mathbf{v})/(\partial p/\partial\theta)$, where $\mathbf{k}$ is a unit vertical vector, ∇_θ is the three-dimensional gradient operator in θ-coordinates, p is the pressure, f is the Coriolis parameter, and g is the acceleration due to gravity. In Juckes (1999) the functions $P_s(\theta)$ and $P_t(\theta)$ were specified as simple analytic functions. Here they are taken from radiosonde profiles. The radiosonde is assumed to be from an unperturbed situation in which the relative vorticity is near zero. The potential vorticity is then given by $(f/\rho)(\mathrm{d}\theta/\mathrm{d}z)$, where ρ is the density and z is height. The resulting profile of potential vorticity defines $P_{s/t}$ for the range of θ values in the stratosphere and troposphere. It is then supposed that the flow is modified by the advection of a cold tropopause anomaly from the north over a certain range of latitudes. The advection brings stratospheric air with potential temperatures below those found in the original profile. The value of $P_s(\theta)$ for these potential temperatures is defined by extrapolating the potential-temperature

* One may envisage circumstances in which enhanced convection may weaken the storm by producing convectively induced downdraughts which, in turn, cool and stabilize the subcloud layer. Emanuel *et al.* (1994) refer to this process as *moist convective damping*. On the other hand, if the middle troposphere is sufficiently moist, as is the case in mature tropical cyclones, downdraughts should be relatively weak and increased convection should cause the storm to intensify (Emanuel 1995).

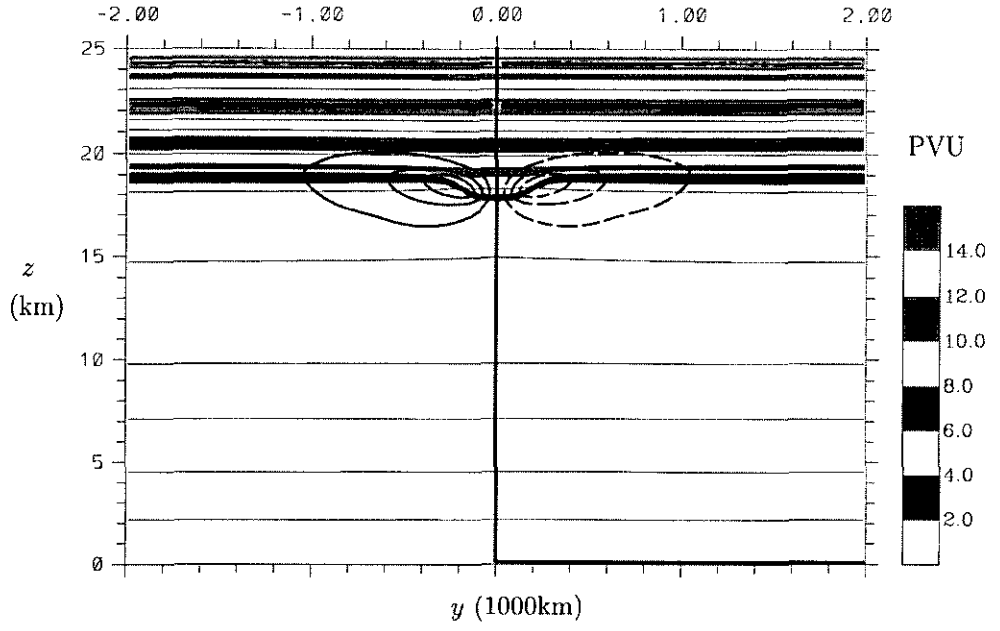

Figure 1. A typical shear-line structure for a width of $y_{\text{trough}} = 200$ km and strength $\theta_{\text{trough}} = 10$ K, from profile B (see Table 1). The thin contours show potential temperature (interval 10 K) and the thicker contours the wind (interval 1 m s^{-1}). The shading shows the potential vorticity.

profile linearly with respect to the logarithm of the pressure. The problem is fully determined when the anomaly in tropopause potential temperature is specified. Here we use the same analytic function as in Juckes (1999), with amplitude θ_{trough} and width y_{trough}.

The resulting shear line is an exact balanced solution of the hydrostatic primitive equations, with a vertical profile at large distances from the anomaly taken from an observed profile and with vanishing isentropic gradients of potential vorticity everywhere except at the tropopause itself.

For each atmospheric profile, ten modified profiles are produced, for anomaly strengths varying from 5 K to 25 K in steps of 5 K and anomaly widths 200 km and 400 km. Figure 1 shows typical shear-line structures for a width of 200 km and strength 10 K. On the scale of this figure, it would appear that there is little ascent of the isentropes at low levels, but what effect there is does have an appreciable effect on the convective destabilization (as shown below).

Figure 2 shows a typical sounding profile. There is a difference between the profile reconstructed from the functions $P_s(\theta)$ and $P_t(\theta)$ and the original profile because of the way the profile near the tropopause is defined. The difference is, however, confined to the stratosphere and the upper two kilometres of the troposphere. The lowest levels of the measured profiles have negative static stability. Rather than attempting to model the processes which maintain this state, the trough model is initialized with a profile in which the lowest levels have been artificially stabilized. This is done by extrapolating from the observed potential temperature at 1 km with the mean of the observed lapse rate between 1 and 2 km. The trough model then calculates the vertical displacements and these are used to generate a perturbed profile. Since the model is initialized with an artificially stabilized profile it will tend to underestimate the vertical displacements

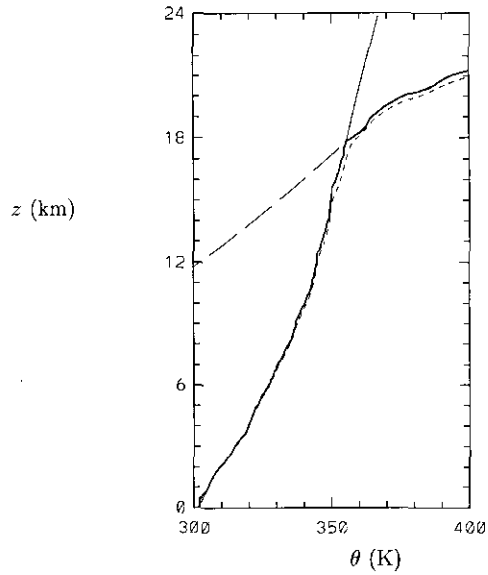

Figure 2. A typical sounding profile. The thick solid line is the measured profile. The thin solid line and the long-dashed line show the tropospheric and stratospheric parts of the profile, respectively, both extrapolated beyond the tropopause so as to define the structure of the anomalously cold stratospheric air or anomalously warm tropospheric air. The final line, short dashes, indicates a profile reconstructed from the functions $P_s(\theta)$ and $P_t(\theta)$ (see text).

and hence provide a lower bound on the degree of destabilization. In practice, however, the vertical displacement in the lowest few kilometres is very small; the dominant effect is the cooling in the upper troposphere, so the degree of underestimation due to this effect is likely to be small. In some of the soundings the foregoing modifications had a significant effect on the calculations of CAPE and CIN whereupon the unmodified values of θ were used for such calculations.

The modified profile is altered further by the introduction of the trough. Figure 3 shows a range of profiles at the centre of a shear line with tropopause potential-temperature anomalies increasing to 25 K in steps of 5 K.

An alternative view of the perturbation is offered in Fig. 4. This figure shows $P_s(\theta)$ and $P_t(\theta)$. Also shown are the background profile, which makes a transition between P_s and P_t at the tropopause, and a perturbed profile, making the transition at a lower potential temperature.

The balanced structures are two dimensional. Juckes (1999) has made a detailed comparison between structures in a primitive-equation model and the small Rossby-number theory. The latter provides quantitatively accurate results up to Rossby numbers of 0.3 and qualitatively similar results at higher Rossby numbers. An advantage of the quasi-geostrophic theory is that the results are not restricted to two-dimensional flows. For general flows, the downward extension of the disturbance depends on the total wave number. This means that a two-dimensional disturbance with horizontal wave numbers $k = 0$, $l = l_0$, say, is equivalent to a three-dimensional disturbance with $k = l = l_0/\sqrt{2}$. That is, in terms of scale, a three-dimensional disturbance must be about $\sqrt{2}$ times larger to have the same downward influence.

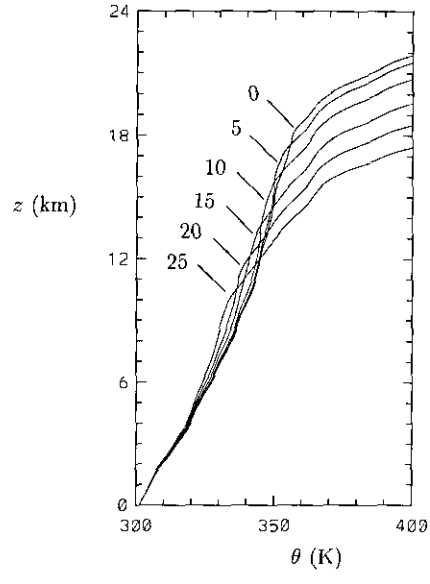

Figure 3. A range of profiles at the centre of a shear line with tropopause potential-temperature anomalies increasing to 25 K in steps of 5 K.

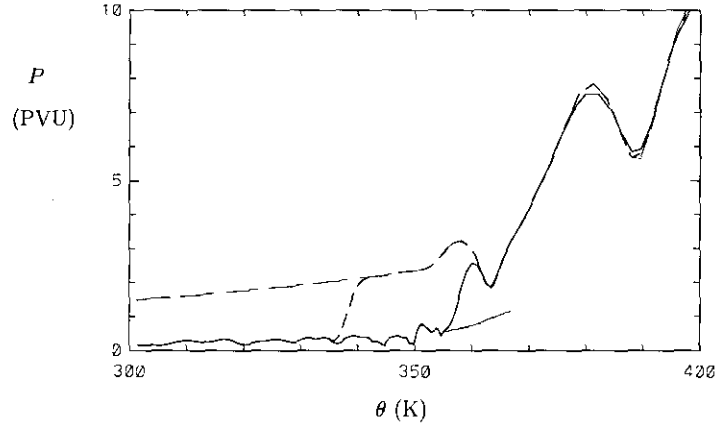

Figure 4. An alternative view of the perturbation, showing $P_s(\theta)$ (thin dashed line), $P_t(\theta)$ (thin solid line), the background profile, which makes a transition between P_s and P_t at the tropopause (thick solid line), and a perturbed profile making the transition at a lower potential temperature (thick dashed line). See text for definition of symbols.

3. THE CALCULATIONS OF CAPE AND CIN

We follow Emanuel (1994) and define the CAPE as the amount of work released by an air parcel of unit mass as it rises from a specified height, z_i, to its uppermost level of neutral buoyancy, z_{LNB}, assuming a particular lifting process. The CIN is defined as the amount of work required to lift the parcel from height z_i to its level of free convection, z_{LFC}, by the same lifting process. Mathematically, the CAPE can be expressed as

$$\mathrm{CAPE}_i = \int_{p_{LNB}}^{p_i} R_d(T_{\rho p} - T_{\rho a})\, \mathrm{d} \ln p, \tag{1}$$

TABLE 1. RADIOSONDE SOUNDINGS FOR WHICH CALCULATIONS ARE CARRIED OUT. VALUES OF CAPE AND CIN (SEE TEXT) ARE CALCULATED ASSUMING *PSEUDO-ADIABATIC ASCENT AND REVERSIBLE ASCENT (VALUES IN BRACKETS)*. LOCAL TIME IS 10 H AHEAD OF UTC IN SAIPAN AND 1 H AHEAD AT EUROPEAN STATIONS.

Sounding	Place	Date	Time UTC	CAPE ($J\,kg^{-1}$)	CIN ($J\,kg^{-1}$)
A	Saipan	4 Aug 1990	0000	2234(1199)	18(43)
B	Saipan	8 Aug 1990	1658	2237(1191)	11(25)
C	Saipan	9 Aug 1990	1058	3347(2157)	2(4)
D	Saipan	15 Aug 1990	1056	2015(898)	1(17)
E	Saipan	20 Aug 1990	1034	1550(1241)	2(9)
F	Lyon	21 July 1992	1200	1384(826)	3(4)
G	Nimes	21 July 1992	1200	1468(785)	16(45)
H	Meiningen	21 July 1992	1200	1403(772)	76(86)
I	Penzing	21 July 1992	1000	596(177)	65(90)

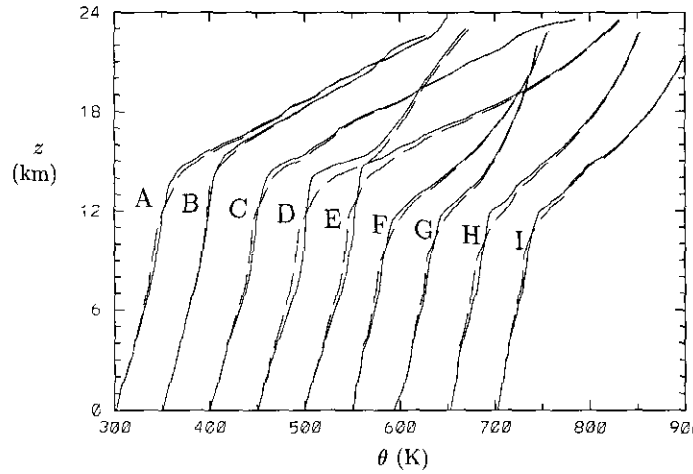

Figure 5. Potential temperature profiles of the nine soundings detailed in Table 1: undisturbed (solid line) and perturbed by a narrow trough with amplitude 15 K (dashed line). Successive profiles are offset by 50 K.

TABLE 2. VALUES OF CAPE AND CIN ($J\,kg^{-1}$) calculated on the assumption of pseudo-adiabatic ascent for the Saipan radiosonde soundings A–E

	A		B		C		D		E	
z_i	$CAPE_i$	CIN_i	$CAPE_i$	CIN_i	$CAPE_i$	CIN_i	$CAPE_i$	CIN_i	$CAPE_i$	CIN_i
500 m	1397	37	1649	24	3223	0	1909	3	1535	0
400 m	2271	17	2271	10	3049	2	1858	3	1699	0
300 m	2329	15	2329	6	3166	4	2056	1	1292	4
200 m	2589	10	2589	8	3653	2	2082	1	1605	4
100 m	2584	11	2584	8	3658	2	2174	0	1622	5
0 m	2694	6	2694	0	4373	0	3149	0	2355	0
average	2234	18	2234	11	3347	2	2015	1	1550	2

See Table 1 for details of soundings.

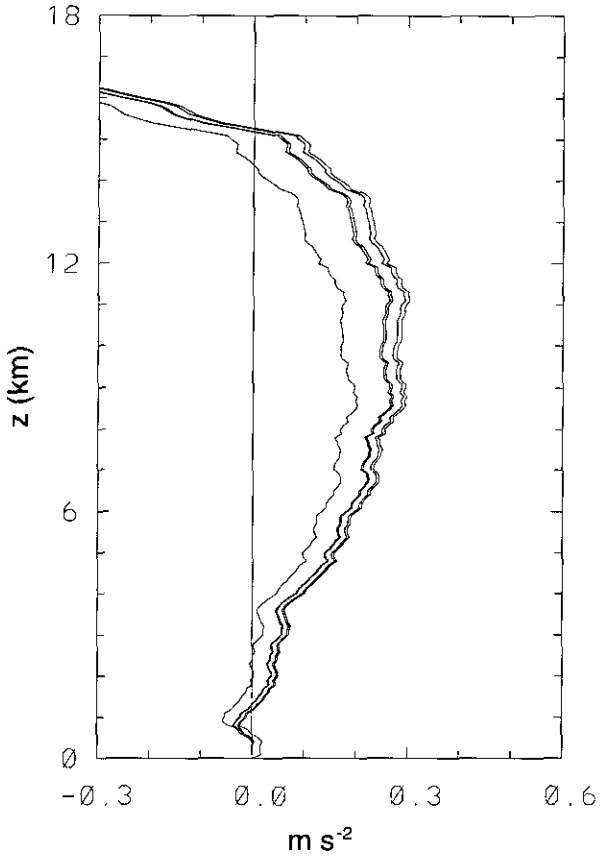

Figure 6. Buoyancy as a function of height for air parcels lifted from the surface and from heights of 100 m to 500 m in steps of 100 m for sounding A assuming pseudo-adiabatic ascent. The rightmost curve is for a parcel lifted from the surface. Curves move to the left as the height of the lifted air parcel increases.

where p_i and p_{LNB} are the pressures at z_i and z_{LNB}, p is an intermediate pressure, $T_{\rho\mathrm{p}}$ and $T_{\rho\mathrm{a}}$ are the density temperatures* of the lifted parcel and the environment at pressure p, and R_{d} is the specific gas constant for dry air. In a similar way, the CIN is defined by

$$\mathrm{CIN}_i = \int_{p_{\mathrm{LFC}}}^{p_i} R_{\mathrm{d}}(T_{\rho\mathrm{p}} - T_{\rho\mathrm{a}})\, \mathrm{d} \ln p, \tag{2}$$

where p_{LFC} is the pressure at z_{LFC}. Typically it is assumed that the lifting occurs *pseudo-adiabatically*, a process in which condensate is assumed to fall out of the parcel as soon as it is formed, or *reversibly*, a process in which all condensate is retained by the ascending parcel. These are two extremes of the real situation where a fraction of condensate falls out and a fraction is retained, and also where some mixing with the environment occurs. Normally, freezing processes are ignored because of uncertainties in the fraction of supercooled water that freezes in a given temperature range (see Williams and Renno (1993)).

Because CAPE and CIN are dependent on the height of the lifted parcel, they do not provide a unique measure of the degree of convective instability and convective

* The density temperature is the temperature of a parcel of cloudy air which has the same density and pressure as a sample of dry air. For a moist unsaturated parcel, the density temperature is just the virtual temperature (see Emanuel (1994)).

TABLE 3. MAXIMUM WIND SPEEDS (M S^{-1}) CORRESPONDING TO BROAD AND NARROW, TROPICAL UPPER-LEVEL *TROUGHS WITH POTENTIAL-TEMPERATURE* AMPLITUDES $\theta_{trough} = 10$ K AND 20 K FOR THE FIVE RADIOSONDE SOUNDINGS A–E

	A	B	C	D	E
Narrow trough					
10 K	9.3	4.1	7.9	20.7	16.2
20 K	18.4	16.1	22.0	35.6	30.1
Broad trough					
10 K	10.9	4.6	9.4	23.7	18.5
20 K	–	19.2	27.0	41.9	35.0

See Table 1 for details of soundings.

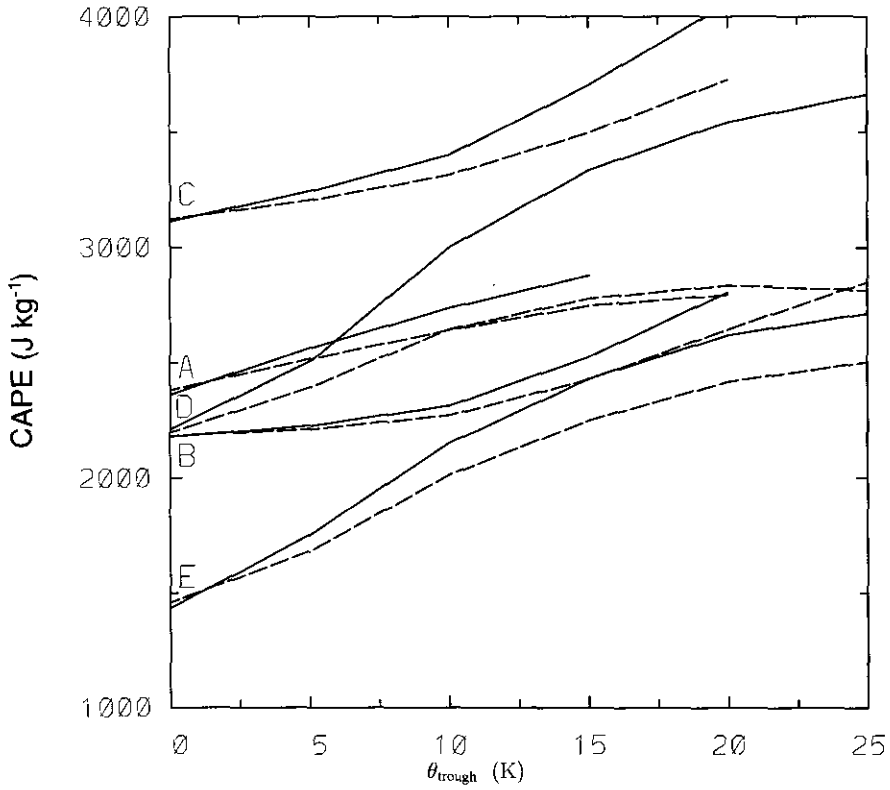

Figure 7. Average CAPE (see text) for each tropical sounding (labelled A–E) for broad troughs (solid lines) and narrow troughs (dashed lines) with amplitudes θ_{trough} of 5 K to 25 K in steps of 5 K and in the absence of a trough ($\theta_{trough} = 0$).

inhibition of the troposphere. The fact that the water-vapour mixing ratio often decreases sharply near the surface results in the CAPE of an air parcel lifted from the surface being much larger than one lifted from a height of 100 m, for example (see Table 2). While part of the sharp near-surface decrease in mixing ratio may be associated with errors in the surface moisture measurement (Betts, personal communication), the subsequent decrease can still lead to a significant decrease in CAPE. To mitigate this problem, many authors calculate a modified sounding by averaging the potential temperature and

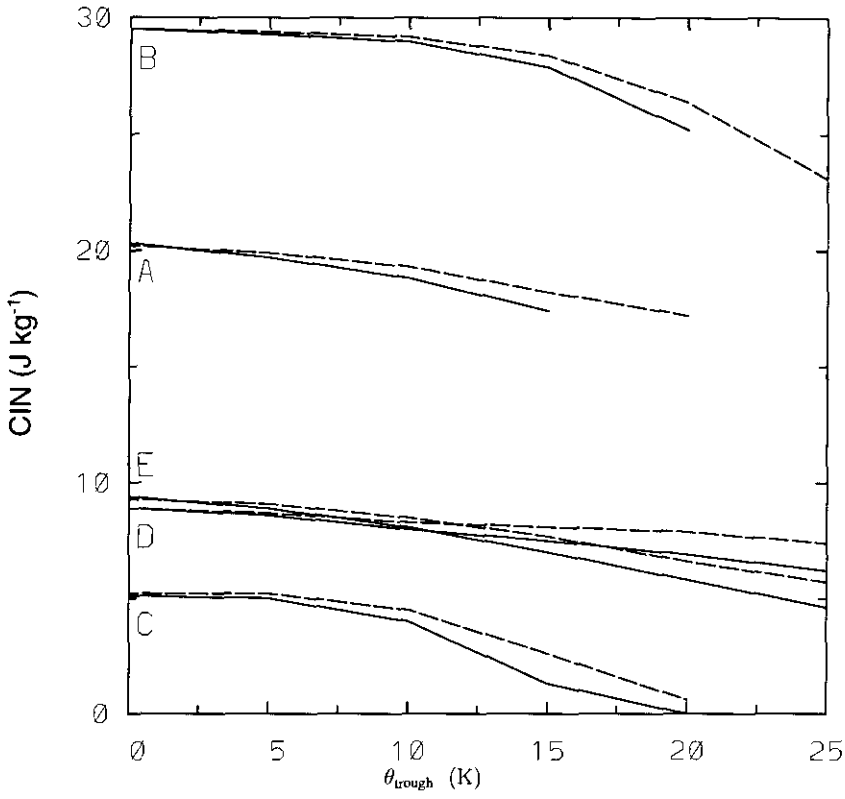

Figure 8. As for Fig. 7, but showing CIN (see text).

mixing ratio over the lowest 500 m, say, and calculate the CAPE and CIN by lifting a surface parcel in the modified sounding. Here we adopt an alternative approach by calculating the CAPE and CIN for parcels lifted from heights of 100 m to 500 m in steps of 100 m and averaging these values to provide a gross measure of the convective instability and convective inhibition.

4. Choice of soundings

Motivated by our interest in the possible effect of convective destabilization by an approaching upper-level trough on tropical cyclone intensification, we have chosen radiosonde soundings for the tropical north-west Pacific as the main basis of this study. Five soundings were selected out of more than 120 carried out on the island of Saipan (15.07°N, 145.43°E) in August 1990 during the Tropical Cyclone Motion Experiment (TCM90). The soundings exhibited a range of typical values of CAPE and CIN. In addition to the tropical soundings, we performed calculations for a few middle-latitude soundings for comparison. The soundings were made on 21 July 1992 over continental Europe ahead of an approaching cold front. On this occasion, a prefrontal squall line developed over southern Germany. The squall-line event is described by Haase-Straub *et al.* (1997). The various soundings, together with the average CAPE and CIN calculated as described in section 3 on the assumption of pseudo-adiabatic ascent and reversible ascent, are detailed in Table 1.

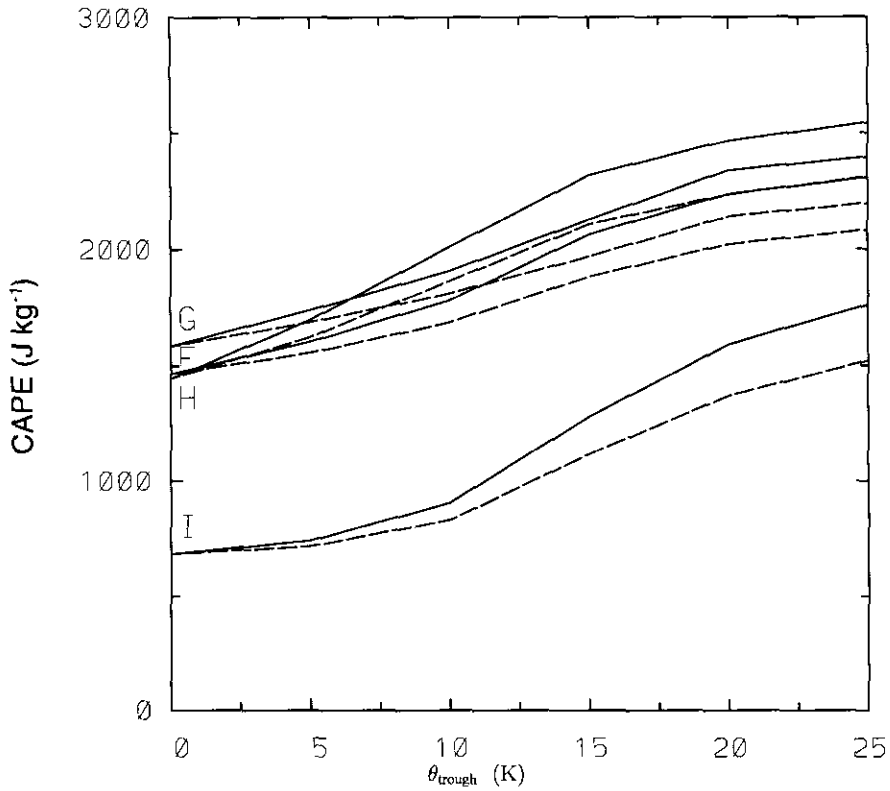

Figure 9. Average CAPE (see text) for each middle-latitude sounding (labelled F–I) for broad troughs (solid lines) and narrow troughs (dashed lines) with amplitudes θ_{trough} of 5 K to 25 K in steps of 5 K and in the absence of a trough ($\theta_{trough} = 0$).

The potential-temperature profiles of the nine soundings are shown in Fig. 5, both undisturbed and after modification by an upper-level trough with half-width 200 km and tropopause potential-temperature anomaly 15 K. The tropical soundings (A–E) are characterized by a high tropopause. Profiles D and E have a marked reduction in lapse rate in the upper troposphere.

Figure 6 shows the buoyancy as a function of height for air parcels lifted from the surface and from heights of 100 m to 500 m in steps of 100 m for sounding A, while Table 2 shows the values of CAPE and CIN for these parcels for soundings A–E. On average the CAPE for parcels lifted from 500 m is only 78% of that for a parcel lifted from 100 m and only 65% of that for a parcel lifted from the surface. In soundings A and B the CIN is three to four times larger than for a parcel lifted from 100 m, while in soundings B–F, parcels lifted from the surface have zero CIN.

5. Results

(*a*) *Tropical upper-level troughs*

Calculations of the average CAPE and CIN are carried out for broad and narrow, tropical upper-level troughs for the five tropical radiosonde soundings with various amplitudes θ_{trough} of 5 K up to 25 K in steps of 5 K and in the absence of a trough ($\theta_{trough} = 0$). The maximum wind speeds associated with some of these troughs are

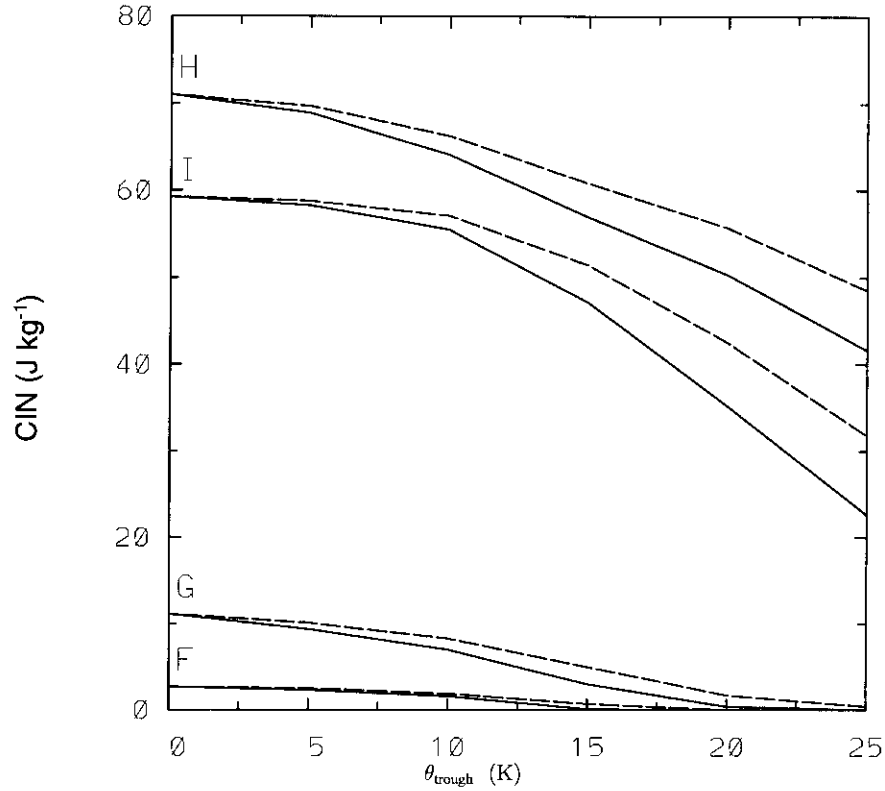

Figure 10. As for Fig. 9, but showing CIN (see text).

detailed in Table 3. The results of these calculations are summarized in Figs. 7 and 8, which show the average CAPE and CIN as functions of θ_{trough}. As expected, the average CAPE increases with increasing trough strength and the increase is larger for a broader trough. The foregoing changes are nonlinear functions of θ_{trough}, varying from sounding to sounding. For example, the increase in CAPE with θ_{trough} for sounding E is relatively large, while that for sounding B is very small for θ_{trough} less than about 10 K, but becomes appreciable as θ_{trough} increases further. Changes in the CIN are generally appreciable for the larger values of θ_{trough}. Maximum increases in CAPE for a broad trough with an amplitude $\theta_{trough} = 20$ K range from 29% for profiles A and B to 83% for profile E, compared with no trough. For a narrow trough the respective values are reduced to 17% for profile A and 72% for profile E. Maximum changes in CIN are also significant. For the broad trough with an amplitude $\theta_{trough} = 20$ K, these range from 15% for profile B to 38% for profile E. For a narrow trough the respective values are reduced to 11% and 29%. We emphasize that the foregoing changes in convective destabilization are upper limits applying to the trough axis; further from the axis, the changes will be proportionately smaller.

There is a limited amount of data on typical trough amplitudes involved in events of tropical-cyclone trough interaction. Figure 2 of Molinari *et al.* (1995) suggests an amplitude of between 5 K and 8 K and half-widths of approximately 300 km, while the panels in Fig. 6 of Molinari *et al.* (1998) show an initially broad trough with a half-width of approximately 800 km and an amplitude of about 5 K (panel a) reducing in size and

increasing in amplitude over a 24 h period to a narrow trough with a half-width of about 200 km and an amplitude of about 10 K (panel c). Both of these cases lie in the lower half of trough amplitudes studied here.

(*b*) *Middle-latitude upper troughs*

The results of the calculations for middle-latitude upper troughs are summarized in Figs. 9 and 10. They are similar to those for the tropical soundings. The average CAPE increases with increasing trough strength and trough breadth, and the change in CAPE with trough breadth is a nonlinear function of θ_{trough}, varying from sounding to sounding. Changes in the CIN are again appreciable for the larger values of θ_{trough}. Maximum increases in CAPE for a broad trough with an amplitude $\theta_{\text{trough}} = 20$ K range from 48% for profile G to 132% for profile I. For a narrow trough the respective values are reduced to 35% for profile G and 100% for profile I. The smallest decrease in CIN for the broad trough with an amplitude $\theta_{\text{trough}} = 20$ K is 29% for profile H, whereas the CIN is completely removed in profile F and nearly removed (a 96% reduction) for profile G. For the narrow trough the smallest decrease in CIN is 22% for profile H and there is an 85% reduction for profile G. Again, the CIN is completely removed in profile F. These changes are significantly larger than for the tropical soundings as might be expected, because the lower troposphere depth in the middle latitudes provides for a greater isentrope displacement for a given trough amplitude and breadth.

6. Discussion and conclusions

We have sought to quantify the extent to which the approach of an upper-level trough can destabilize the atmosphere to moist convection. We have shown that the changes in CAPE are significant in the Tropics (up to 83% for the soundings examined) and even larger in the middle latitudes (up to 130%). Changes in CIN can be appreciable also, and in some cases the CIN may be completely removed. Of course, it is not necessary that the CIN be completely removed for deep convection to be initiated. The calculated changes in CAPE and CIN represent the maximum degree of destabilization that occurs at the trough axis; and the local destabilization decreases with increasing distance from this axis. The calculations here are for idealized trough structures. In future studies it would be of interest to extend them to cases of observed troughs, both in the Tropics and in middle latitudes.

The calculations were motivated by a desire to understand the interaction between a tropical cyclone and an approaching upper-level trough, but they fall short of addressing this much more difficult problem directly. As they stand, the calculations would be relevant only to the outer regions of the cyclone where the air is subsaturated. The challenge remains to understand how such changes in CAPE and CIN would affect the tropical cyclone itself, and to determine how important such changes would be. One would need also to take account of the changes in structure and reduction in scale of the upper trough as a result of the interaction (see e.g. Molinari *et al.* 1995). To address these questions will require the use of a tropical-cyclone model.

Acknowledgement

This research was supported by the US Office of Naval Research through Grant No. N00014-95-1-0394.

REFERENCES

Danielsen, E. F. 1968 Stratospheric–tropospheric exchange based on radioactivity, ozone and potential vorticity. *J. Atmos. Sci.*, **25,** 502–518

Eliassen, A. and Kleinschmidt, E. 1957 Dynamic Meteorology. *Handbuch der Physik.*, **48,** 1–154

Emanuel, K. A. 1994 *Atmospheric Convection.* Oxford University Press, Oxford

1995 The behavior of a simple hurricane model using a convective scheme based on subcloud layer entropy equilibrium. *J. Atmos. Sci.*, **52,** 3960–3976

Emanuel, K. A., Neelin, J. D. and Bretherton, C. S. 1994 On large-scale circulations in convecting atmospheres. *Q. J. R. Meteorol. Soc.*, **120,** 1111–1143

Haase-Straub, S. P., Hagen, M., Hauf, T., Heimann, D., Peristeri, M. and Smith, R. K. 1997 The squall line of 21 July 1992 in southern Germany: An observational case study. *Beitr. Phys. Atmos.*, **70,** 147–165

Hoskins, B. J., McIntyre, M. E. and Robertson, A. W. 1985 On the use and significance of isentropic potential vorticity maps. *Q. J. R. Meteorol. Soc.*, **111,** 877–946

Juckes, M. 1999 The structure of idealized upper-tropospheric shear lines. *J. Atmos. Sci.*, **56,** 2830–2845

Molinari, J., Skubis, S. and Vollaro, D. 1995 External influences on hurricane intensity. Part III: Potential vorticity structure. *J. Atmos. Sci.*, **52,** 3593–3606

Molinari, J., Skubis, S., Vollaro, D., Alsheimer, F. and Willoughby, H. E. 1998 Potential vorticity analysis of tropical cyclone intensification. *J. Atmos. Sci.*, **55,** 2632–2644

Reed, R. J. 1955 A study of a characteristic type of upper-level frontogenesis. *J. Meteorol.*, **12,** 226–237

Williams, E. and Renno, N. 1993 An analysis of the conditional instability of the tropical atmosphere. *Mon. Weather Rev.*, **121,** 21–36